

Upstream Influence and Peak Heating in Hypervelocity Shock Wave/Boundary-Layer Interaction

S. G. Mallinson,* S. L. Gai,† and N. R. Mudford‡
University of New South Wales, Canberra ACT 2601, Australia

Two important characteristics of separated flow, namely, the scale of interaction and the peak heat transfer, have been examined under high-enthalpy, hypersonic conditions. Experimental data have been obtained in a free-piston shock tunnel using a compression corner model. The data are examined in terms of established perfect gas theories, and are seen to be in reasonable agreement with these theories and also with data from perfect gas experiments. This indicates that, for the present conditions, the real gas effects on separation and reattachment are small.

Nomenclature

| | |
|-------------|---|
| C | = Chapman–Rubesin constant, $(\mu/\mu_\infty)(T_\infty/T)$ |
| d | = leading-edge thickness |
| h | = enthalpy |
| h_r | = recovery enthalpy, $h_0 + 0.5(Pr^{1/2} - 1)U_\infty^2$ |
| k_R | = specific recombination rate coefficient, $AT^{-\omega}$ |
| k_{R0} | = $2k_RT^\omega$ |
| L | = upstream plate fetch |
| Le | = Lewis number |
| L_{pk} | = growth length of the reattaching boundary layer to the location of peak heating |
| l_s | = length of the separated region |
| l_u | = upstream influence |
| M | = Mach number |
| m | = pressure gradient parameter |
| n | = index of peak pressure ratio |
| Pr | = Prandtl number |
| p | = pressure |
| q_w | = heat transfer |
| Re_x | = Reynolds number based on distance x , $\rho_\infty U_\infty x / \mu_\infty$ |
| Re_∞ | = unit Reynolds number, $\rho_\infty U_\infty / \mu_\infty$ |
| R_0 | = universal gas constant |
| St | = Stanton number, $q_w / [\rho_\infty U_\infty (h_r - h_\infty)]$ |
| T | = temperature |
| U | = velocity |
| x | = distance from leading edge |
| α_0 | = oxygen dissociation fraction |
| β_s | = shear-layer detachment angle |
| γ_f | = frozen ratio of specific heats |
| δ | = boundary-layer thickness |
| δ_s | = shear-layer thickness at reattachment |
| ζ | = Damkohler number, τ_d / τ_r |
| θ_w | = corner angle |
| μ | = viscosity |
| ρ | = density |
| τ_d | = characteristic particle diffusion time |

| | |
|----------------|---|
| τ_r | = characteristic reaction time |
| $\bar{\chi}_0$ | = hypersonic viscous interaction parameter, $M_0^3(C^*/Re_{x_0})^{1/2}$ |
| ω | = exponent in recombination rate |

Subscripts

| | |
|----------|--|
| e | = conditions at the edge of the boundary layer |
| fp | = flat-plate value |
| g | = value for gas phase |
| pk | = peak value |
| s | = value for surface material |
| w | = conditions at the wall |
| o | = value at the beginning of the interaction, x_0 |
| 0 | = reservoir conditions |
| ∞ | = conditions in the freestream |

Superscript

| | |
|---|--|
| * | = evaluated at the Eckert reference enthalpy |
|---|--|

Introduction

SHOCK wave/boundary-layer interaction can seriously degrade the performance of air-breathing engines. The phenomenon can result in inlet unstart,¹ engine choking,² and cause localized high pressure and heat loads on the engine structure.^{3–10} Although shock-induced separation has been considered extensively under cold hypersonic conditions (see Refs. 3 and 5 for excellent reviews of this subject), it has received little attention at high-enthalpy conditions that will typically be encountered in hypersonic flight, in general, and by supersonic combustion ramjets (scramjets), in particular.

Previous studies of separation and the attendant reattachment process in reacting flows have been mainly numerical in nature.^{2,11–20} To summarize these studies, when the bulk real gas effect is exothermic (e.g., vibrational relaxation, recombination, and combustion), the scale of separation is found to increase, whereas for endothermic processes (e.g., vibrational excitation and dissociation) a decrease in the scale of separation is observed. It is also reasonable to say that whatever differences exist between the peak heat transfer for reacting and nonreacting flows appear to depend significantly upon the catalytic of the reattachment surface.

The picture is somewhat more complicated when we consider the sparse experimental studies. Stalker and Rayner²¹ performed experiments with a compression corner set at incidence in a free-piston shock tunnel. They found the separated length to be well predicted by perfect gas theory, even for total enthalpies up to 25 MJ kg⁻¹. Rayner²² noticed some differences at higher enthalpies, but these may be attributed to the contamination of the test flow by cold helium driver gas.²³ Krek et al.²⁴ and Davis et al.²⁵ have recently found a substantial

Received Sept. 28, 1995; revision received March 16, 1996; accepted for publication April 8, 1996. Copyright © 1996 by the authors. Published by the American Institute of Aeronautics and Astronautics, Inc., with permission.

*Associate Lecturer, The Australian Defence Force Academy, School of Aerospace and Mechanical Engineering; currently at the Department of Aeronautics, Imperial College of Science, Technology and Medicine, London SW7 2BY, UK. Member AIAA.

†Associate Professor, The Australian Defence Force Academy, School of Aerospace and Mechanical Engineering. Associate Fellow AIAA.

‡Lecturer, The Australian Defence Force Academy, School of Aerospace and Mechanical Engineering.

Table 1 Reservoir and freestream conditions

| Condition | $h_{0\infty}$ MJ kg ⁻¹ | $p_{0\infty}$ MPa | $T_{0\infty}$ K | p_{∞} kPa | T_{∞} K | ρ_{∞} g m ⁻³ | u_{∞} km s ⁻¹ | M_{∞} | Re_{∞} $\times 10^{-5}$ m ⁻¹ | $\gamma_{f\infty}$ | α_0 |
|-----------|--------------------------------------|----------------------|--------------------|---------------------|-------------------|--------------------------------------|------------------------------------|--------------|---|--------------------|------------|
| B | 19.0 | 22.2 | 8400 | 0.99 | 1160 | 2.60 | 5.47 | 7.5 | 3.10 | 1.45 | 0.8 |
| D | 13.7 | 22.2 | 7200 | 0.99 | 940 | 3.43 | 4.72 | 7.5 | 4.08 | 1.43 | 0.4 |
| G | 2.83 | 22.4 | 2400 | 0.73 | 160 | 16.0 | 2.28 | 9.1 | 32.2 | 1.40 | 0.0 |

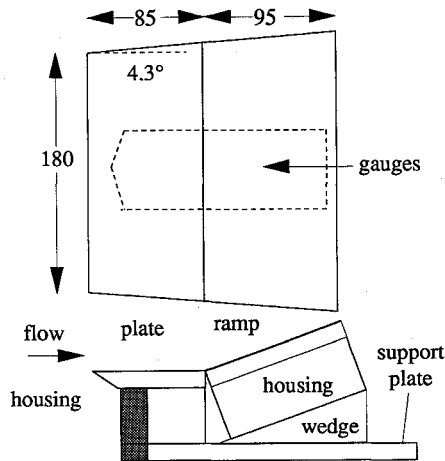


Fig. 1 Schematic of the model (side plates not shown).

difference in the separated length at high enthalpy for flows over axisymmetric configurations tested in the large free-piston shock tunnel facilities at the DLR-Göttingen and Graduate Aeronautical Laboratories-California Institute of Technology (GALCIT), respectively. Given the relatively high values of Reynolds numbers external to the boundary layer in their experiments, the results may also have been affected by transition to turbulence near separation.

For the present investigation, a compression corner model has been chosen as it has been previously studied under a wide range of perfect gas conditions and, also, it is typical of engine inlet and fuel injector configurations for scramjets.²⁶⁻²⁹ This article will examine the data in terms of established perfect gas theories to look at the possible role of real gas effects in hypersonic separation and reattachment. It must be noted that the flow was laminar throughout,³⁰ and thus, any real gas effects should not be masked by the competing effects of transition to turbulent flow.

Experimental Details

Experiments have been conducted using the Australian National University's free-piston shock tunnel, T3. Details of its operation are to be found elsewhere.^{31,32} The test gas was air. Three conditions were employed, designated B, D, and G.³³ These conditions have total enthalpies ranging from 2.8 MJ kg⁻¹ for condition G to 19.0 MJ kg⁻¹ for condition B, giving freestream speeds of 2.3–5.5 km s⁻¹, respectively. The non-isentropic expansion through the nozzle gives a freestream flow that is partially dissociated. For condition B, there was a high level of atomic oxygen in the freestream; for condition D, there was a moderate level of atomic oxygen in the freestream; whereas the freestream for condition G contained no atomic oxygen. Note that the levels of atomic nitrogen were negligible for all three conditions and that there were small amounts of nitric oxide (NO) in the freestream for conditions B and D (approximately 3 and 1%, respectively). The maximum enthalpy was chosen so that there was sufficient time to establish steady separated flow³⁴ before driver gas contamination became significant.²³ Details of the procedure used to determine the reservoir and freestream conditions, as shown in Table 1, are given elsewhere.^{30,35}

The model (see Fig. 1) was composed of a flat plate and a ramp plate that rest upon gauge housings. The corner angle

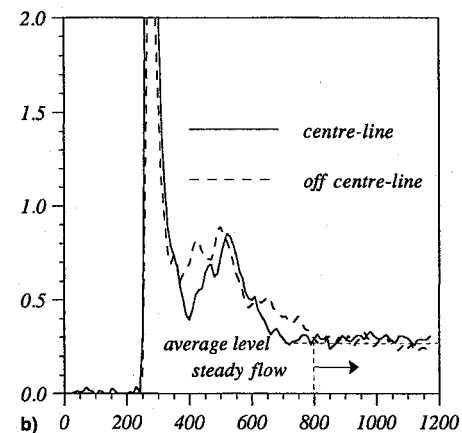
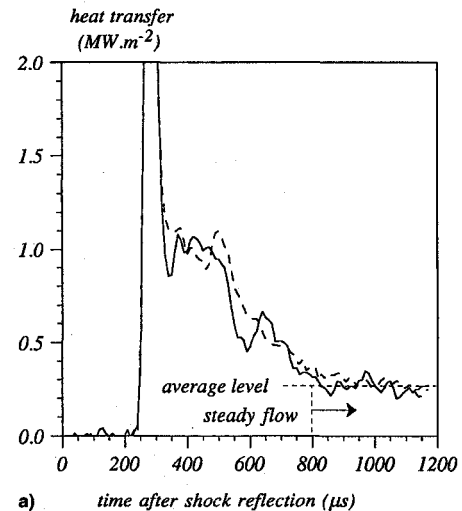


Fig. 2 Heat transfer signals for centerline and off centerline locations within the separated region: a) with and b) without side fences.

was adjusted by inserting wedges beneath the housings. Ramp angles considered in the present study were $\theta_w = 10, 15, 18$, and 24 deg, along with the datum case of flat-plate flow, that is, $\theta_w = 0$ deg. The junction beneath the flat plate and the ramp plate was sealed from below to avoid leakage problems. Interference of the test surface flow by the flow from beneath the model surface was prevented by side plates. The Reynolds number based on the leading-edge thickness Re_d was less than 100. This satisfies the criterion for sharpness proposed by Stollery,³⁶ and therefore, bluntness effects may be neglected.

An axisymmetric conical nozzle, with a throat diameter of 12.7 mm, exit diameter of 304.8 mm, and a half-angle of 7.5 deg, was employed in the present experiments. A pitot survey of the nozzle showed the flow divergence over the model length to be approximately 1 deg. This will induce a slight pressure gradient of the form $U_e \sim x^m$. The value of m was calculated using an expression from Ref. 37 and found to be approximately equal to 0.01 for all three conditions. The flow divergence effects are therefore considered small.

The compression corner is a nominally two-dimensional flow problem. However, spillage or outflow from the top of

the model, particularly near the separated region, may result in significant three-dimensional effects.³⁸ To examine the three dimensionality of the present flows, experiments were conducted with and without side fences, which prevent outflow from the upper surface of the model. The heat transfer was measured within the separated region at on- and off-axis locations. The results, shown in Fig. 2, indicate that the addition of side fences did not have any significant effect, and that the heat transfer both on- and off-axis is very similar in the levels and in the time variation. This would seem to suggest that for the present experiments, the flow in the model midspan may be considered approximately two dimensional.

The pressure and heat transfer distributions were measured using PCB 113M165 pressure transducers and in-house manufactured coaxial chromel-alumel (type K) surface junction thermocouples. Details of their calibration are to be found elsewhere.^{30,35} Some flow visualization data were obtained using a Mach-Zehnder interferometer. The interferograms were analyzed using fast two-dimensional Fourier transform techniques developed at the Australian National University.³⁹

Upstream Influence

It is not always a simple task to determine the l_s from flow visualization data, and in many instances, the data are not available. The l_u may be defined as the distance upstream of the inviscid shock location where the pressure and heat transfer distributions first deviate from the flat-plate distributions (i.e., the distributions observed in the absence of the shock). This parameter varies in practically the same manner as the length of separation and is therefore a useful means of characterizing the scale of the interaction. An example of how l_u is determined from the pressure and heat transfer distributions is shown in Fig. 3. From both the pressure and the heat transfer distributions, the value of l_u is given by $l_u = L - x_0 \approx 85 - 54 = 31$ mm.

It has been shown^{30,35} that the upstream influence for a perfect gas flow may be described using the following relationship:

$$l_u/\delta = F[(M_0\theta_w)^2/\bar{\chi}_0] \quad (1)$$

Equation (1) may be obtained from consideration of the governing parameters for hypersonic flow over an inclined flat plate.⁴¹ The variation of l_u as expressed by Eq. (1) is similar to that for the length of l_s found by Katzer,⁴² which was supported by the triple-deck theory for separated flows. Kumar⁴³ has employed essentially the same parameters to correlate a wide range of cold hypersonic shock wave/boundary-layer interaction data. It is interesting to note that the incipient separation condition^{44,45} is of the same form as Eq. (1).

When real gas effects become significant, the interaction may be affected by 1) a change in the incoming boundary-layer thickness, 2) a change in the shock strength, 3) real gas effects in the recirculating region, and 4) a change in the boundary-layer thickness near or after reattachment. The last of these should not significantly affect the upstream influence, but may alter the heating levels on the ramp face. This point will be examined in the next section.

The boundary-layer thickness for nonequilibrium flow differs from the perfect gas value by an amount that depends upon the level of nonequilibrium in the boundary layer.^{30,46} For dissociation-dominated boundary-layer flow, the boundary-layer thickness would be reduced, whereas for recombination-dominated flow, the thickness would be increased. According to Eq. (1), this would mean the upstream influence would be reduced for dissociation-dominated flows and increased for recombination-dominated flows. This is in agreement with previous numerical studies.^{11-14,16-20} The high-enthalpy boundary layers in the present study were found to be essentially chemically frozen.^{30,46} This means that the upstream influence

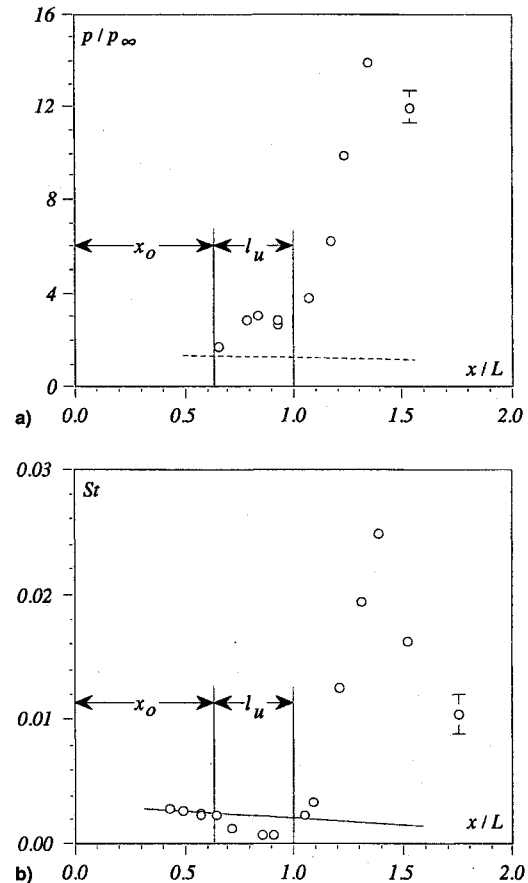


Fig. 3 Determination of l_u and x_0 : a) pressure distribution; b) heat transfer distribution, corner located at $x/L = 1.0$. \circ , experimental data (condition B, $\theta_w = 24$ deg, see Ref. 35); ———, weak interaction theory⁴⁶; ———, reference enthalpy theory, modified to include the effect of freestream dissociation.³³

should not be significantly affected by real gas effects in the boundary layer for the present high-enthalpy conditions.

The shock angle, and therefore shock strength, may be reduced because of dissociation and vibrational excitation through the separation shock. The distance required for this to happen, however, would be many body lengths. Significant nonequilibrium effects of this nature are to be expected only for wedge angles much larger than those used here.⁴⁷ Even then, the difference between frozen and equilibrium shock angles is only a few degrees,^{48,49} and so the effect on the pressure would be small.

Lastly, let us consider the possible real gas effects on the recirculating region. If the length scale for the nonequilibrium chemical processes l_{chem} is of the same order as the scale of separated region, then it becomes an additional variable in Eq. (1). For frozen flow, reaction times are much larger than the characteristic flow time and $l_{chem}/\delta \rightarrow \infty$. For equilibrium flow, reaction times are much less than the characteristic flow time and $l_{chem}/\delta \rightarrow 0$. The chemical length scale is therefore not a determining variable for the scale of interaction when the flow is frozen or in equilibrium. When the flow is in equilibrium, the length of the separated region will still be affected by the change in boundary-layer thickness as discussed in the previous paragraph. The boundary layer for the present high-enthalpy conditions is essentially chemically frozen, which indicates that the chemical length scale is much larger than the boundary-layer thickness. Thus it is not expected that relaxation in the recirculating region would affect the scale of interaction.

The upstream influence for separated flows for conditions B, D, and G is compared in Fig. 4 using the form of Eq.

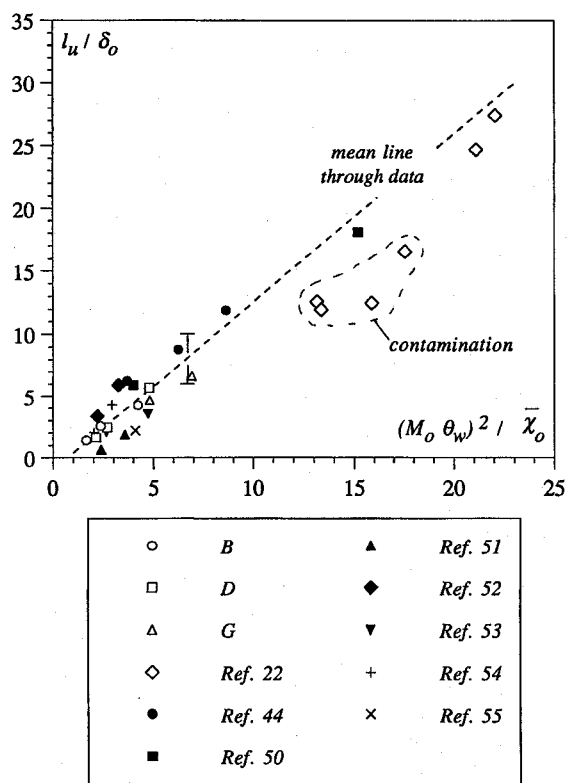


Fig. 4 Upstream influence in hypersonic laminar compression corner flow.

(1). Also shown are the experimental data from the low-enthalpy^{44,50-55} and high-enthalpy²² experiments, along with an average line through the data. The data from the other experiments are known to be for laminar flow throughout the separated region. The flow was deemed separated if either the pressure distribution had a plateau, the heat transfer showed a rounded minimum, the skin friction decreased below zero, or the flow visualization data revealed a separated region. The value of the boundary-layer thickness was calculated using an expression given in Refs. 35 and 46, which was in good agreement with data from low- and high-enthalpy experiments. The low- and high-enthalpy data from the present experiments correlate well in the form of Eq. (1) as do the low-enthalpy data from the other experiments. Some of the data from the high enthalpy experiments of Ref. 22 lay significantly below the other data. These points were obtained at enthalpies in excess of 25 MJ kg⁻¹ in the T3 facility, for which it is known that there are unacceptable levels of driver gas contamination.²³

From Fig. 4, the high-enthalpy flows appear to behave as a perfect gas. The observation from a previous study,⁵⁶ that the upstream influence in the present high-enthalpy flows was less than that for perfect gas flows, was because of the use of an incorrect correlating parameter.

Peak Heating on the Ramp Face

The relationship between the peak heating and peak pressure near reattachment is often presented in terms of the two ratios q_{pk}/q_{fp} and p_{pk}/p_{fp} . Neumann⁵⁷ and Holden³ gave expressions of the form

$$q_{pk}/q_{fp} = (p_{pk}/p_{fp})^n \quad (2)$$

where different values of n are applicable to laminar and turbulent interactions. Taking $n = 0.7$ gives the best agreement with laminar data, whereas $n = 0.85$ seems to be the most appropriate value for turbulent flows. This expression has been successfully applied to data from a wide range of shock wave/boundary-layer experiments.^{3,5,57}

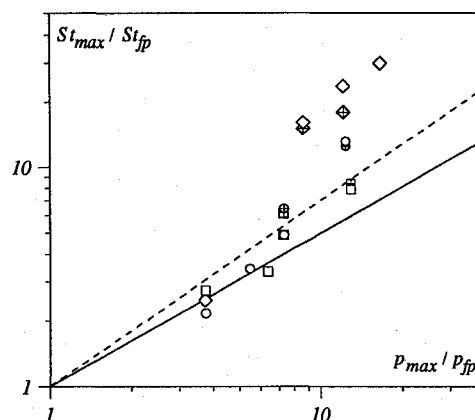


Fig. 5 Correlation of peak heating vs peak pressure. ○, condition B; □, condition D; ◇, condition G; —, Neumann-Holden correlation, Eq. (2), laminar flow, $n = 0.7$; —, Neumann-Holden correlation, Eq. (2), turbulent flow, $n = 0.85$; crossed symbols, values from Simeonides et al.⁶³ relation, Eq. (6), laminar flow, $s = 0.5$.

Data from the present experiments are shown in Fig. 5. Note that the ratio of peak-to-flat-plate heat transfer is expressed in terms of the corresponding Stanton number ratio to eliminate any small shot-to-shot differences between the flow conditions. Also shown are the predictions for laminar and turbulent flow given by the Neumann-Holden correlation, Eq. (2). It can be seen that for the low-pressure ratios, there exists a good agreement between the laminar theory and experiment, although the scatter is of the same order as the difference between the laminar and turbulent predictions. For the experiments with the higher peak pressures, the measured peak heat transfer lies above even the prediction for turbulent flows. For these experiments, the heat transfer traces do not exhibit the characteristic unsteadiness observed in transitional and turbulent flows.⁴³ Given the high Mach number and low Reynolds numbers of the flows examined here, it would seem reasonable to assume that the elevated heating is not because of turbulent flow.

The elevated heating levels may be because of the heat added to the flow by recombination of the atomic oxygen that is present in the freestream for conditions B and D. Atomic nitrogen is present in negligible amounts ($<10^{-5}\%$), and so its effect will be small. The relative importance of recombination may be determined by calculating ζ , which is a ratio of the characteristic times for diffusion and reaction. For chemically frozen flows $\zeta \ll 1$, for flows in chemical equilibrium $\zeta \gg 1$, and for flows in nonequilibrium $\zeta = \mathcal{O}(1)$. The Damkohler numbers for gas-phase and surface-catalyzed recombination in the flow on the ramp face have been calculated using the following expressions⁵⁸:

$$\zeta_s = \frac{4x}{U_e} \frac{k_{R_0}}{T_e^{\omega+2}} \left(\frac{p}{R_0} \right)^2 = \frac{\tau_d}{\tau_r} \quad (3)$$

$$\zeta_s = \frac{Pr p_w k_w (2x)^{1/2}}{Le (p_e U_e \mu_e C_w)^{1/2}} = \frac{\tau_d}{\tau_{r,w}} \quad (4)$$

where the gas-phase reaction rate has been taken as³³

$$k_R = 1.13 \times 10^{20} T^{-3/2} \text{ cm}^6 \text{ g}^{-1} \text{ mol}^{-2} \text{ s}^{-1} \quad (5)$$

whereas the surface reaction rate has been taken from Ref. 59 as $k_w \approx 5 \text{ m s}^{-1}$. Calculations of ζ have been performed for the high corner angles of conditions B and D only, as the condition G flow has negligible levels of atomic species in the freestream. The distance x in Eqs. (3) and (4) is assumed to have its origin at the corner. This is reasonable as previous results^{46,60} have found the flat-plate configuration to be chemically frozen to recombination. The calculation was performed at $x = 47.5 \text{ mm}$ (i.e., at halfway along the ramp face).

Table 2 Gas-phase and surface-catalyzed Damkohler numbers for conditions B and D halfway along the ramp face

| Condition | θ_w , deg | ζ_g | ζ_s |
|-----------|------------------|----------------------|-----------|
| B | 18 | 5.6×10^{-3} | 1.2 |
| | 24 | 4.5×10^{-3} | 1.6 |
| D | 18 | 1.5×10^{-2} | 1.3 |
| | 24 | 1.2×10^{-2} | 1.7 |

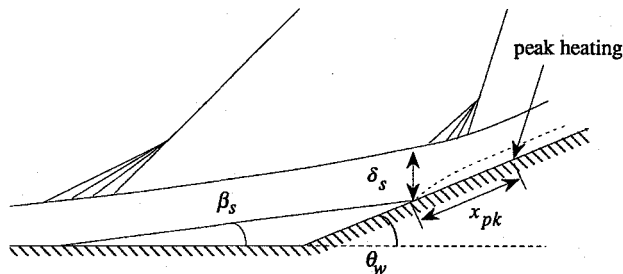


Fig. 6 Determination of δ_s and β_s (after Bushnell and Weinstein⁶⁵).

The results of the calculations, shown in Table 2, reveal that the gas-phase recombination is still quite frozen on the ramp, yet the surface-catalyzed recombination seems to be in non-equilibrium. The chemical potential enthalpy for conditions B and D is 2.5 and 1.2 MJ kg⁻¹, respectively, which represents 15 and 10% of the recovery enthalpy for these flows. Thus, recombination could explain at most 10–15% of the differences between the experiment and the Neumann–Holden correlation, Eq. (2), observed in Fig. 5. However, much larger differences than this are evident for some of the flows. It is also important to note that for the higher than expected heating levels experienced at condition G, this explanation will not be applicable.

Similar unusually high heating levels have also been observed in connection with stagnation point heat transfer on blunt bodies,^{61,62} where the mechanism has been described in terms of surface roughness. Such a mechanism may also be possible here as the reattachment point is similar to a stagnation point. However, this phenomenon is difficult to quantify.

Simeonides et al.⁶³ noticed that at high-peak pressure ratios, the length scale of the reattaching boundary layer influenced the peak heating. They successfully compared a wide range of peak heating data with the following expression, which may be obtained from the generalized reference enthalpy theory⁶⁴:

$$q_{pk}/q_{tp} = (p_{pk}/p_{tp})^{1-s} (x_{pk}/L_{pk})^s \quad (6)$$

Here, $s = 0.5$ for laminar interactions and $s = 0.2$ for turbulent interactions. The value of L_{pk} may be calculated using⁶⁵

$$L_{pk} = \delta_s / \sin(\theta_w - \beta_s) \quad (7)$$

The values of δ_s and β_s may be obtained from flow visualization data, where available. A schematic of this procedure is shown in Fig. 6.

The predicted peak heat transfer ratios based on Eq. (6) are shown in Fig. 5 as crossed symbols. As is clear, the high-pressure ratio data that lay above both the laminar and turbulent predictions from the Neumann–Holden correlation [Eq. (2)], are in reasonable agreement with the predictions from Eq. (6). It would therefore seem that the reduction in the scale of the reattaching boundary layer explains the higher than originally expected heating levels and thus a recourse to roughness or real gas effects or transition to turbulent flow appears unnecessary. Note that the scatter is of the same order as the experimental uncertainty of $\pm 15\%$.

Further examination of Eq. (6) reveals that variations in the reattachment scale $\sim L_{pk}$ will alter the peak heat transfer. As mentioned in the previous section, the real gas effects may affect the boundary-layer thickness near reattachment. For flows where the overall real gas effect is endothermic, a smaller δ_s and, therefore, a higher peak heat transfer could be expected. This has been predicted by several numerical investigations.^{11,12,14,16,18,20} For flows where the overall real gas effect is exothermic, the boundary layer will have a greater thickness, and so a lower value of peak heating could be expected. Grumet et al.¹⁹ found for exothermic flows that the peak heat transfer was actually increased. The reason for this is not clear, but one may speculate that the exothermic processes added sufficient heat to the flow to exceed the loss because of the thicker boundary layer.

Conclusions

The separation and reattachment of a high-enthalpy, hypersonic laminar boundary layer has been examined for the case of compression corner flow.

It was found that the scale of the interaction was well described by a simple expression that was consistent with the triple deck theory of separated flow, and that the differences between high- and low-enthalpy flows were negligible for the present experiments. It was also demonstrated that any real gas effects on separation would be mainly because of the changes in the boundary-layer thickness upstream of the interaction or nonequilibrium effects in the reversed flow region. The results from numerical studies of real gas separating flows are consistent with the present hypothesis.

The peak heat transfer on the ramp face was well described by the Neumann–Holden correlation for perfect gas flows when the peak pressure ratio was small. For higher peak pressures, the reattachment process was more severe, promoting higher heat transfer rates. The peak heating, in this case, was in fair agreement with an expression based on the generalized reference enthalpy method, which included the scale of the reattaching boundary layer as a variable. Using this expression, it was also possible to reconcile the higher heat transfer rates from numerical predictions of real gas shock wave/boundary-layer interactions.

From these results, it may be concluded that the real gas effects on separation and reattachment are negligible for the present flows. Compression corner experiments are planned by other researchers for the large free-piston shock tunnel facilities at the DLR–Göttingen²⁴ and GALCIT²⁵ and it will be interesting to see whether the results from these tests show any real gas effects.

Acknowledgments

The authors would like to thank the Department of Physics and Theoretical Physics, Australian National University, for providing the interferogram analysis package. They also thank P. M. Walsh for assistance with the experiments, and J. W. Morton and R. R. Boyce for advice on the flow visualization and interferogram analysis.

References

- Hawkins, W. R., and Marquart, E. J., "Two-Dimensional Generic Inlet Unstart Detection at Mach 2.5–5.0," AIAA Paper 95-6019, April 1995.
- Weidner, E. H., and Drummond, J. P., "Numerical Study of Staged Fuel Injection for Supersonic Combustion," *AIAA Journal*, Vol. 20, No. 10, 1982, pp. 1426–1431.
- Hankey, W. L., Jr., and Holden, M. S., "Two Dimensional Shock Wave—Boundary Layer Interactions in High Speed Flows," AGARD-ograph 203, June 1975.
- Morgan, R. G., and Stalker, R. J., "Shock Tunnel Measurements of Heat Transfer in a Model Scramjet," *Journal of Spacecraft and Rockets*, Vol. 23, No. 5, 1986, pp. 470–475.
- Délery, J., "Shock/Shock and Shock-Wave/Boundary-Layer Interactions in Hypersonic Flows," AGARD Rept. 761, Pt. 9, June 1989.

- ⁶Bakos, R., Tamagno, J., Trucco, R., Rizkalla, O., Chinitz, W., and Erdos, J. I., "Mixing and Combustion Studies Using Discrete Orifice Injection at Hypervelocity Flight Conditions," *Journal of Propulsion and Power*, Vol. 8, No. 6, 1992, pp. 1290-1296.
- ⁷Brescianini, C. P., and Morgan, R. G., "Numerical Modelling of Wall-Injected Scramjet Experiments," *Journal of Propulsion and Power*, Vol. 9, No. 2, 1993, pp. 169-175.
- ⁸Singh, D. J., Trexler, C. A., and Young, J. A. H., "Three-Dimensional Simulation of a Translating Strut Inlet," *Journal of Propulsion and Power*, Vol. 10, No. 2, 1994, pp. 191-197.
- ⁹Ishiguro, T., Takaki, R., Mitani, T., and Hiraiwa, T., "Three-Dimensional Analysis of Scramjet Nozzle Flows," *Journal of Propulsion and Power*, Vol. 10, No. 4, 1994, pp. 540-545.
- ¹⁰Messitt, D. G., Nagamatsu, H. T., and Myrabo, L. N., "Combined Numerical and Experimental Investigation of a 2-D Scramjet Inlet at Mach Numbers from 10 to 25," AIAA Paper 95-6020, April 1995.
- ¹¹Drummond, J. P., and Weidner, E. H., "Numerical Study of a Scramjet Engine Flowfield," *AIAA Journal*, Vol. 20, No. 9, 1982, pp. 1182-1187.
- ¹²Ballaro, C. A., and Anderson, J. D., Jr., "Shock Strength Effects on Separated Flows in Non-Equilibrium Chemically Reacting Air Shock Wave/Boundary Layer Interaction," AIAA Paper 91-0250, Jan. 1991.
- ¹³Kordulla, W., Riedelbauch, S., Brenner, G., and Prinz, U., "Hypersonic Viscous Flow Simulations," *Fluid Dynamics Research*, Vol. 10, 1992, pp. 451-468.
- ¹⁴Brenner, G., and Prinz, U., "Numerical Simulation of Chemical and Thermal Nonequilibrium Flows After Compression Shocks," AIAA Paper 92-2879, July 1992.
- ¹⁵Yungster, S., "Numerical Study of Shock-Wave/Boundary-Layer Interactions in Premixed Combustible Gases," *AIAA Journal*, Vol. 30, No. 10, 1992, pp. 2379-2387.
- ¹⁶Grasso, F., and Leone, G., "Chemistry Effects in Shock Wave Boundary Layer Interaction," edited by R. Brun and A. A. Chikhaoui, *Aerothermochemistry of Spacecraft and Associated Hypersonic Flows*, Jouve, Paris, 1992, pp. 220-227.
- ¹⁷Leyland, P., Perrel, F., Vos, J. B., and Bergmann, M., "A Family of Multiblock Codes for Computational Aerothermodynamics: Application to Complete Vehicle Hypersonic Flows," AIAA Paper 93-3042, July 1993.
- ¹⁸Brenner, G., Gerhold, T., Hannemann, K., and Rues, D., "Numerical Simulation of Shock/Shock and Shock-Wave/Boundary-Layer Interactions in Hypersonic Flows," *Computers Fluids*, Vol. 22, Nos. 4-5, 1993, pp. 427-439.
- ¹⁹Grumet, A., Anderson, J. D., Jr., and Lewis, M. J., "Numerical Study of the Effects of Wall Catalysis on Shock Wave/Boundary Layer Interaction," *Journal of Thermophysics and Heat Transfer*, Vol. 8, No. 1, 1994, pp. 40-47.
- ²⁰Oswald, J., Demargne, A., and Bousquet, J.-M., "Hypersonic Laminar Computations of Separated Flows with Account of Real Gas Effects," AIAA Paper 95-2271, June 1995.
- ²¹Stalker, R. J., and Rayner, J. P., "Shock Wave-Laminar Boundary Layer Interaction at Finite Span Compression Corners," *Shock Waves and Shock Tubes*, edited by D. Bershader and R. Hanson, Stanford Univ. Press, Stanford, CA, 1985, pp. 509-515.
- ²²Rayner, J. P., "Boundary Layer Separation and Thermal Choking," Ph.D. Dissertation, Australian National Univ., Canberra, Australia, April 1973.
- ²³Crane, K. C. A., and Stalker, R. J., "Mass-Spectrometric Analysis of Hypersonic Flows," *Journal of Physics D: Applied Physics*, Vol. 10, April 1977, pp. 679-695.
- ²⁴Krek, R. M., Eitelberg, G., and Beck, W. H., "Hyperboloid Flare Experiments in the HEG," 20th International Symposium on Shock Waves, California Inst. of Technology, Pasadena, CA, July 1995.
- ²⁵Davis, J., Sturtevant, B., and Muylaert, J., "Experiments on the Halis Axisymmetric Configuration in the T5 Hypervelocity Shock Tunnel," 20th International Symposium on Shock Waves, California Inst. of Technology, Pasadena, CA, July 1995.
- ²⁶Lewis, M. J., "Designing Hypersonic Inlets for Bow Shock Location Control," *Journal of Propulsion and Power*, Vol. 9, No. 2, 1993, pp. 313-321.
- ²⁷Fathauer, B. W., and Rogers, R. C., "A Computational Investigation of Fuel Mixing in a Hypersonic Scramjet," AIAA Paper 93-2994, July 1993.
- ²⁸Wadawadigi, G., Tannehill, J. C., Buelow, P. E., and Lawrence, S. L., "Three-Dimensional Upwind Parabolized Navier-Stokes Code for Supersonic Combustion Flowfields," *Journal of Thermophysics and Heat Transfer*, Vol. 7, No. 4, 1993, pp. 661-667.
- ²⁹Lachner, R., Hönig, R., Hoßfeld, H.-C., Magrini, G. L., and Kappler, G., "One-Dimensional Model of the Chemically Reacting Flow in a Supersonic Combustion Chamber," *Zeitschrift für Flugwissenschaften und Weltraumforschung*, Vol. 19, Feb. 1995, pp. 34-40.
- ³⁰Mallinson, S. G., "Shock Wave/Boundary Layer Interaction at a Compression Corner in Hypervelocity Flows," Ph.D. Dissertation, Univ. of New South Wales, Canberra, Australia, Dec. 1994.
- ³¹Stalker, R. J., "Development of a Hypervelocity Wind Tunnel," *Aeronautical Journal*, Vol. 76, June 1972, pp. 374-384.
- ³²Gai, S. L., "Free Piston Shock Tunnels: Developments and Capabilities," *Progress in Aerospace Sciences*, Vol. 29, 1992, pp. 1-41.
- ³³East, R. A., Stalker, R. J., and Baird, J. P., "Measurements of Heat Transfer to a Flat Plate in a Dissociated High-Enthalpy Laminar Air Flow," *Journal of Fluid Mechanics*, Vol. 97, No. 4, 1980, pp. 673-699.
- ³⁴Mallinson, S. G., and Gai, S. L., "Establishment of Laminar Separated Flows in a Free-Piston Shock Tunnel," *Aerothermochemistry of Spacecraft and Associated Hypersonic Flows*, edited by R. Brun and A. A. Chikhaoui, Jouve, Paris, 1992, pp. 368-373.
- ³⁵Mallinson, S. G., Gai, S. L., and Mudford, N. R., "High Enthalpy, Hypersonic Compression Corner Flow," AIAA Paper 95-0155, Jan. 1995.
- ³⁶Stollery, J. L., "Viscous Interaction Effects on Re-Entry Aerothermodynamics: Theory and Experimental Results," *Aerodynamic Problems of Hypersonic Vehicles*, edited by R. C. Pankhurst, Vol. 1, AGARD Lecture Series 42, 1972.
- ³⁷Cohen, C. G., and Reshotko, E., "Similar Solutions for the Compressible Laminar Boundary Layer with Heat Transfer and Pressure Gradient," NACA Rept. 1293, 1956.
- ³⁸Rudy, D. H., Thomas, J. L., Kumar, A., Gnoffo, P. A., and Chakravarthy, S. R., "Computation of Laminar Hypersonic Compression-Corner Flows," *AIAA Journal*, Vol. 29, No. 7, 1991, pp. 1108-1113.
- ³⁹Boyce, R. R., Morton, J. W., Houwing, A. F. P., Mundt, C., and Bone, D. J., "CFD Validation Using Multiple Interferometric Views of Three Dimensional Shock Layer Flows over a Blunt Body," AIAA Paper 94-0282, Jan. 1994.
- ⁴⁰Anderson, J. D., Jr., *Hypersonic and High Temperature Gas Dynamics*, McGraw-Hill, New York, 1989.
- ⁴¹Stollery, J. L., "Hypersonic Viscous Interaction on Curved Surfaces," *Journal of Fluid Mechanics*, Vol. 43, No. 3, 1970, pp. 497-511.
- ⁴²Katzer, E., "On the Lengthscales of Laminar Shock/Boundary-Layer Interaction," *Journal of Fluid Mechanics*, Vol. 206, 1989, pp. 477-496.
- ⁴³Kumar, D., "Hypersonic Control Flap Effectiveness," Ph.D. Dissertation, Cranfield Univ., Cranfield, England, UK, 1995.
- ⁴⁴Needham, D. A., and Stollery, J. L., *Hypersonic Studies of Incipient Separation and Separated Flows*, Vol. 4, Pt. 1, AGARD Conference Proceedings, 1966, pp. 89-119.
- ⁴⁵Inger, G. R., "Scaling of Incipient Separation in High Speed Laminar Flows," *Aeronautical Journal*, Vol. 98, June-July 1994, pp. 227-231.
- ⁴⁶Mallinson, S. G., Gai, S. L., and Mudford, N. R., "The Boundary Layer on a Flat Plate in Hypervelocity Flow," *Aeronautical Journal*, Vol. 100, No. 994, 1996, pp. 135-141.
- ⁴⁷Kewley, D. J., and Hornung, H. G., "Non-Equilibrium Dissociating Nitrogen Flow over a Wedge," *Journal of Fluid Mechanics*, Vol. 64, No. 4, 1974, pp. 725-736.
- ⁴⁸Capiiaux, R., and Washington, M., "Nonequilibrium Flow Past a Wedge," *AIAA Journal*, Vol. 1, No. 3, 1963, pp. 650-660.
- ⁴⁹Pandolfi, M., Arina, R., and Botta, N., "Nonequilibrium Hypersonic Flows over Corners," *AIAA Journal*, Vol. 29, No. 2, 1991, pp. 235-241.
- ⁵⁰Putnam, L. E., "Investigation of Effects of Ramp Span and Deflection Angle on Laminar Boundary-Layer Separation at Mach 10.03," NASA TN D-2833, May 1965.
- ⁵¹Holden, M. S., "Theoretical and Experimental Studies of Laminar Flow Separation on Flat Plate-Wedge Compression Surfaces in the Hypersonic Strong Interaction Regime," U.S. Air Force-Aeronautical Research Lab. Rept. 67-0112, 1967.
- ⁵²Lewis, J. E., Kubota, T., and Lees, L., "Experimental Investigation of Supersonic Laminar, Two-Dimensional Boundary-Layer Separation in a Compression Corner with and Without Cooling," *AIAA Journal*, Vol. 6, No. 1, 1968, pp. 7-14.
- ⁵³Holden, M. S., and Moselle, J. R., "Theoretical and Experimental Studies of the Shock Wave-Boundary Layer Interaction on Compression Surfaces in Hypersonic Flow," U.S. Air Force-Aeronautical Research Lab. Rept. 70-0002, 1970.
- ⁵⁴Bloy, A. W., and Georgeff, M. P., "The Hypersonic Laminar Boundary Layer near Sharp Compression and Expansion Corners,"

Journal of Fluid Mechanics, Vol. 63, 1974, pp. 431–447.

⁵⁵Grasso, F., Leone, G., and Délerly, J. M., "Validation Procedure for the Analysis of Shock-Wave/Boundary-Layer Interaction Problems," *AIAA Journal*, Vol. 32, No. 9, 1994, pp. 1820–1827.

⁵⁶Mallinson, S. G., Gai, S. L., and Mudford, N. R., "Shock Wave/Boundary Layer Interaction in High Enthalpy Compression Corner Flow," *Shock Waves @ Marseille*, edited by R. Brun and L. Z. Dumitrescu, Vol. 1, 1993, Springer-Verlag, Berlin, pp. 87–92.

⁵⁷Neumann, R. D., "Special Topics in Hypersonic Flow," *Aerodynamic Problems of Hypersonic Vehicles*, edited by R. C. Pankhurst, Vol. 1, AGARD Lecture Series 42, 1972.

⁵⁸Chung, P. M., "Chemically Reacting Nonequilibrium Boundary Layers," *Advances in Heat Transfer*, edited by J. P. Hartnett and T. F. Irvine Jr., Vol. 2, Academic, 1965, pp. 109–270.

⁵⁹Goulard, R., "On Catalytic Recombination Rates in Hypersonic Stagnation Heat Transfer," *Jet Propulsion*, Vol. 28, No. 11, 1958, pp. 737–745.

⁶⁰Gai, S. L., Mudford, N. R., Roberts, G. T., and Mallinson, S. G., "Effects of Catalytic and Boundary Layer Reactions on Surface Heat Flux in Hypersonic High Enthalpy Flows," 20th International Symposium on Shock Waves, California Inst. of Technology, Pasadena, CA, July 1995.

CA, July 1995.

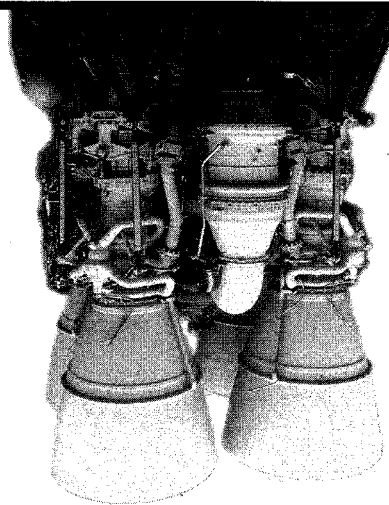
⁶¹Richards, B. E., and Enkenhus, K. R., "Hypersonic Testing in the VKI Long Shot Free Piston Tunnel," *AIAA Journal*, Vol. 8, No. 6, 1970, pp. 1020–1026.

⁶²Gai, S. L., Lyons, P. R. A., Baird, J. P., and Sandeman, R. J., "Some Heat Transfer Measurements over a Sphere-Cone in High Enthalpy Non-Equilibrium Flow," *Shock Waves and Shock Tubes*, edited by D. Bershader and R. Hanson, Stanford Univ. Press, Stanford, CA, 1985, pp. 649–656.

⁶³Simeonides, G., Haase, W., and Manna, M., "Experimental, Analytical, and Computational Methods Applied to Hypersonic Compression Ramp Flows," *AIAA Journal*, Vol. 32, No. 2, 1994, pp. 301–310.

⁶⁴Neumann, R. D., and Hayes, J. R., "Introduction to Aerodynamic Heating Analysis of Supersonic Missiles," *Tactical Missile Aerodynamics*, edited by M. J. Hemsch and J. N. Neilsen, Vol. 104, Progress in Astronautics and Aeronautics, AIAA, New York, 1986, pp. 421–481.

⁶⁵Bushnell, D. M., and Weinstein, L. M., "Correlation of Peak Heating for Reattachment of Separated Flows," *Journal of Spacecraft and Rockets*, Vol. 5, No. 9, 1968, pp. 1111, 1112.



Spacecraft Propulsion

Charles D. Brown

This valuable new textbook describes those subjects important to conceptual, competitive stages of propulsion design and emphasizes the tools needed for this process.

The text begins with a discussion of the history of propulsion and outlines various propulsion system types to be discussed such as cold gas systems, monopropellant systems, bipropellant systems, and solid systems. Included with the text is PRO: AIAA Propulsion Design Software which allows the reader to proceed directly from understanding into professional work and provides the accuracy, speed, and convenience of personal computing. Also, the software contains conversion routines which make it easy to move back and forth between English and Metric systems.

A recommended text for professionals and students of propulsion.

CONTENTS:

Introduction • Theoretical Rocket Performance • Propulsion Requirements • Monopropellant Systems • Bipropellant Systems • Solid Rocket Systems • Cold Gas Systems • PRO: AIAA Propulsion Design Software • Propulsion Dictionary • Propulsion Design Data • Subject Index

1995, 350 pp, illus, Hardback

ISBN 1-56347-128-0

AIAA Members \$59.95

Nonmembers \$74.95

Order #: 28-0(945)



American Institute of Aeronautics and Astronautics

Publications Customer Service, 9 Jay Gould Ct., P.O. Box 753, Waldorf, MD 20604
Fax 301/843-0159 Phone 1-800/682-2422 8 a.m. – 5 p.m. Eastern

Sales Tax: CA and DC residents add applicable sales tax. For shipping and handling add \$4.75 for 1–4 books (call for rates for higher quantities). Orders under \$100.00 must be prepaid. Foreign orders must be prepaid and include a \$20.00 postal surcharge. Please allow 4 weeks for delivery. Prices are subject to change without notice. Returns will be accepted within 30 days. Non-U.S. residents are responsible for payment of any taxes required by their government.